

The effect of the waves on magnetic confinement is seen to be given by the parallel ponderomotive force, which is no longer the gradient of a scalar and, importantly now, depends on the sign of $B_0 \partial_s (B_0^{-1} |E_\omega|^2) = \nabla \cdot (\hat{e}_{\parallel} |E_\omega|^2)$. The apparent perpendicular thermal broadening can also be estimated as $\Delta\mu \approx (q^2/mB_0) \sum_\omega |E_\omega|^2 / 2(\omega - \Omega)^2$. Both of these results are needed to self-consistently evaluate wave plugging in open systems.

In conclusion, the spatial effects of low-amplitude waves on a plasma have been described by a consistent kinetic perturbation theory. A true ponderomotive-force term arises in second-order kinetic theory, but only for electromagnetic waves, for which the time average of products of terms arising from fluctuating electric fields with terms arising from the associated fluctuating magnetic fields produces an effective force in the direction of $\nabla |E_\omega|^2$. The purely electrostatic part of the fluctuations generates a time-average effect best described by a velocity-space diffusion operator, which for the low-velocity nonresonant part of the distribution produces a local, apparent temperature increase in the direction of \vec{E} . Some care is required in comparing velocity moments of \bar{f} with macroscopic fluid quantities. Both velocity moments of \bar{f} and the time average of products of fluctuating quantities must be considered; for example, in one dimension, the

time-averaged fluid velocity is given by

$$\bar{u} = \langle \bar{n} \rangle^{-1} \int dv v \bar{f} [1 - (2q^2/m^2) \sum_\omega \omega^{-4} |\partial_x E_\omega|^2].$$

Finally, the treatment here has been for the nonresonant part of the distribution function with particle velocities less than the phase velocity of the waves; similar methods may also be applied in the opposite limit.

This work was supported by the U. S. Energy Research and Development Administration under Contracts No. AT-(04-3)-1018 and No. EY-76-C-02-2277*000.

¹R. Z. Sagdeev and A. A. Galeev, *Nonlinear Plasma Theory* (Benjamin, New York, 1969), Chap. II.

²W. E. Drummond, *Phys. Fluids* **7**, 816 (1964).

³J. F. Drake, P. K. Kaw, Y. C. Lee, G. Schmidt, C. S. Liu, and M. N. Rosenbluth, *Phys. Fluids* **17**, 778 (1974).

⁴D. B. Chang, *Phys. Fluids* **7**, 1980 (1964).

⁵B. Bezzerides and D. F. DuBois, *Phys. Rev. Lett.* **34**, 1381 (1975); B. Bezzerides, D. F. DuBois, D. W. Forslund, and E. L. Lindman, *Phys. Rev. Lett.* **38**, 495 (1977).

⁶H. Motz and C. J. H. Watson, *Adv. Electron.* **23**, 153 (1967).

⁷R. J. Hastie, J. B. Taylor, and F. A. Haas, *Ann. Phys. (N.Y.)* **41**, 302 (1967).

Simulations of Nonlinearly Stabilized Beam-Plasma Interactions

H. L. Rowland and K. Papadopoulos

Naval Research Laboratory, Washington, D. C. 20375, and University of Maryland, College Park, Maryland 20742

(Received 25 July 1977)

Computer simulations of the kinetic warm-beam instability with finite-mass ions are reported. It is shown that strong turbulence, including Langmuir collapse, stabilized the beam-plasma instability before quasilinear plateau formation. This process decreases significantly the beam-plasma coupling and increases the propagation distance in accordance with laboratory and space observations.

The interaction of a warm electron beam with a plasma in the kinetic regime has been the classic example of the application of quasilinear theory.¹ According to this theory the beam plasma instability is stabilized in a time $t \approx (n_p/n_b)\omega_e^{-1}$ (n_p and n_b are the plasma and beam density) with the beam forming a quasilinear plateau, while releasing one-third of its energy to plasma waves and one-third to sloshing energy of the ambient plasma. However, laboratory beam-plasma in-

teraction experiments indicated much longer energy-coupling time scales than that predicted above.² This coupled with the observation of beams propagating over extremely large distances in space³ without any significant plateau formation has led to an extensive search for a nonlinear mechanism that can stabilize the beam-plasma instability on a time scale faster than that required for plateau formation. It was not till recently⁴ that a strong-turbulence theory with

respect to wave interactions was applied to the problem. It was shown^{4,5} that when $W_R/n_p T_e > (k_0 \lambda_D)^2$ ($k_0 \lambda_D = v_{Te}/v_b$, W_R is the wave energy in resonance with the beam, v_b is the beam velocity, v_{Te} is the background electron thermal velocity) processes similar to the parametric instabilities occurring in laser-pellet absorption can operate with time scales faster than the beam-growth time and transfer wave energy, contrary to the weak-turbulence theory, to large wave numbers ($k \gg k_0$) where they can be absorbed by forming long electron tails in the background plasma. It should be noted that these processes, predominantly called the modulational or oscillating two-stream instability or Langmuir collapse, result in the existence of nonlinearly coupled electron and ion waves, and their description requires the allowance of dynamic ion response. The phenomena disappear when the ions are considered as an immobile neutralizing background. Because of its complexity, the theory as presented in Refs. 4 and 5 involved several assumptions. To remedy this we present here the first numerical simulations which conclusively demonstrate the role of strong-turbulence nonlinear stabilization mechanisms and the fact that beams can propagate over times much longer than quasilinear theory predicts without forming a plateau. The emphasis in this Letter is on the fundamental physical processes involved. More theoretical details can be found in previous work,⁴⁻⁷ while detailed scalings will be presented elsewhere.

Before describing the results of our simulations, we comment briefly on previous numerical work on the subject. Particle simulations^{8,9} of the resonant beam-plasma instability have confirmed quasilinear considerations.⁹ However, in these simulations the ions were treated as an immobile ($m_i = \infty$) neutralizing background; nonlinear strong-turbulence effects which involve ion dynamics such as discussed in Refs. 4-7 are excluded at the outset. On the other hand, particle simulations^{10,11} of the hydrodynamic stage (cold beam) of the beam-plasma instability were performed with finite-mass ions which demonstrated that the trapping of beam electrons is the stabilizing mechanism while strong-turbulence parametric processes controlled the subsequent absorption and redistribution of the wave energy. At this stage we should comment on the reason that finite-mass-ion simulations in the kinetic regime were not performed earlier. As is well known in particle simulations, because of the finite number of ions per Debye length, we expect a density

fluctuation level substantially higher than in actual collisionless plasmas. This results in the appearance of an anomalous high-frequency resistivity ν^* at ω_e , as discussed by Dawson and Oberman.¹² While this does not affect the hydrodynamic instability because of its reactive nature, it does not allow the growth of the kinetic instability as long as $\nu^* > \gamma$, where γ is the growth rate. It turns out that to achieve $\gamma > \nu^*$ one had to use so many particles that the simulation was not feasible. In fact all attempts at simulating the resonant beam-plasma instability failed to show any growth. In order to correct this deficiency, while at the same time keeping the dynamic response of the ions, we developed a hybrid code where the ions are represented as a charged one-dimensional ideal fluid with phenomenological damping. This is allowed for our purposes since it has been shown¹³ that such a description is equivalent to a kinetic treatment for the ions, as far as the heavily damped ion acoustic modes (ion acoustic quasimodes) are concerned. That is, both conserve energy and momentum in a similar manner in the transfer process. More details on the scheme as well as a discussion of its limitations will be presented elsewhere.

In order to distinguish between the strong-turbulence and the quasilinear effects we performed a series of simulations. We discuss here in detail the results of two runs and will summarize the results of the rest in Fig. 4. For these two runs the initial conditions are the same; the only difference between the two simulations is that in one an ion mass of $128m_e$ is used, while in the other the ions are infinitely massive. As noted above, by setting the ion mass to infinity we eliminate nonlinear parametric interactions. By comparing the two simulations we expect to isolate the effects of nonlinear interactions on the warm-beam-plasma system.

For the two comparison runs, the system length is $1024 \lambda_D$ and the particle density is 40 particles per λ_D . The initial parameters are $n_b/n_p = 0.0025$, $v_b/v_{Te} = 41$, $\Delta v_b/v_{Te} = 8.3$, where Δv_b and v_{Te} are the beam and plasma thermal velocities.

Figure 1(a) shows the field energy of the modes in resonance with the beam. Until approximately $700\omega_{pe}^{-1}$, the two simulations are the same. By this time in the run with finite-mass ions, the beam-driven modes have started to act as a pump to drive up shorter-wavelength ion fluctuations and electron plasma oscillations. This acts to remove energy from the beam modes. When the loss rate exceeds the growth rate due to the beam,

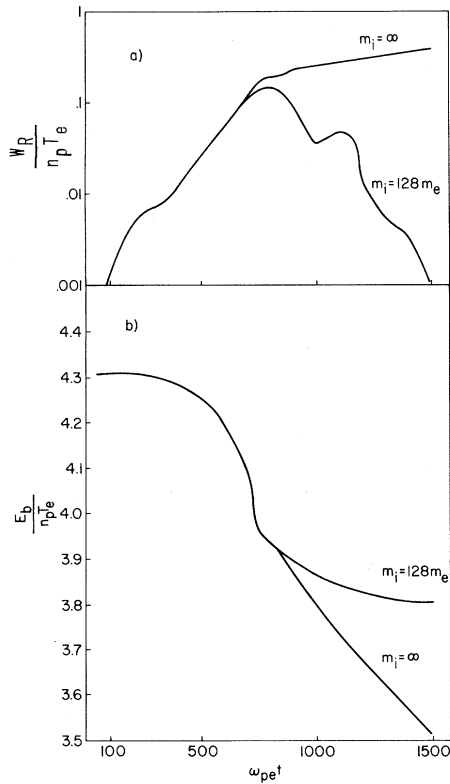


FIG. 1. Time development of kinetic beam instability as seen in computer simulation with and without ion dynamics. (a) Energy in electrostatic waves in resonance with beam and (b) kinetic energy of beam. Non-linear parametric instabilities act to damp resonant waves and limit beam-energy loss.

the modes stabilize and then damp. By reducing W_R the energy loss rate of the beam is reduced. This can be clearly seen in Fig. 1(b) which shows the total kinetic energy of the beam particles. In the simulation with finite-mass ions we can see the decoupling of the beam.

In Fig. 2 we compare the electron velocity distribution for the two runs. The vertical scale is logarithmic. In the case with infinite-mass ions, the beam has formed a flat plateau with the lower-velocity side propagating down in velocity space. This is in qualitative and quantitative agreement with quasilinear theory as presented by Ivanov and Rudakov.¹⁴ In the simulation with ion dynamics, the distribution is markedly different. The parametric instability has transferred the energy in the electron plasma oscillations to shorter-wavelength modes. These modes are in resonance with the background plasma and heat the electrons by forming symmetric superthermal tails. The beam has not lost any

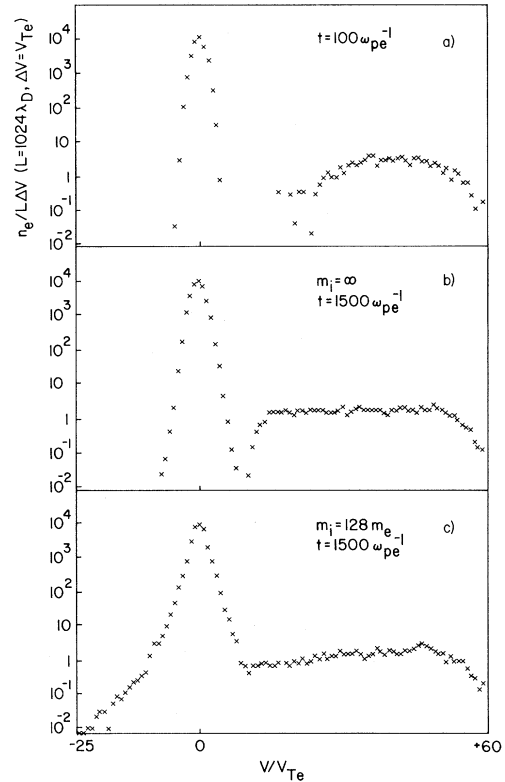


FIG. 2. Velocity distribution for background electrons and beam. (a) Initial distribution; (b) without ion dynamics formation of quasilinear plateau; (c) with ion dynamics beam retains positive slope and superthermal tails formed on background. Note that vertical scale is logarithmic.

energy for approximately $300\omega_{pe}^{-1}$ but it still has a positive slope. This can be seen more clearly in Fig. 3 which replots the beam distributions on a linear scale.

Having confirmed the fundamental idea of the nonlinear stabilization, we performed a series of seven simulations with finite-mass ions, to determine the scaling of the maximum wave energy and the beam energy loss with the growth rate γ (Fig. 4). The two points marked with a *B* represent runs with a particle beam. For the other points the beam was modeled in the code by causing the longest-wavelength mode to be resistively unstable. The numerical results confirm the expected analytic scaling⁴ of $W_{R, \max} / n_p T_{e0}$. The beam energy loss can be computed as

$$\begin{aligned} \Delta E_b &= 2[W_{R, \max} + 2\gamma W_{R, \max} \int_0^\infty dt \exp(-2\gamma_p t)] \\ &\approx 4W_{R, \max}, \end{aligned}$$

where γ_p is the nonlinear rate at which energy

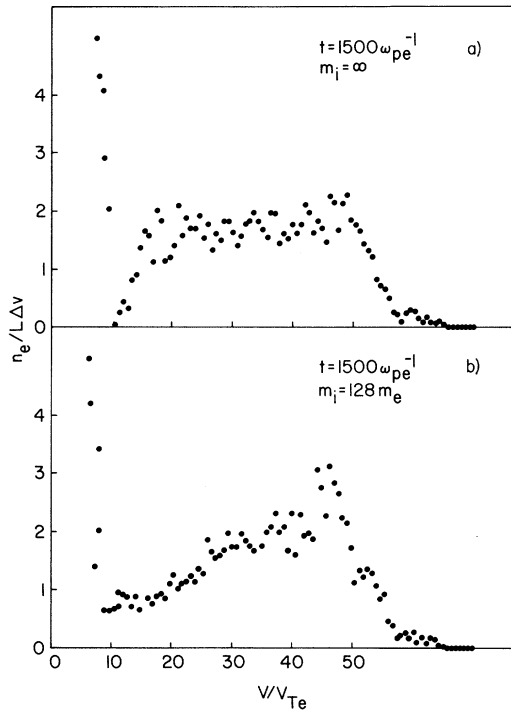


FIG. 3. Velocity distribution plotted on linear graph. With nonlinear stabilization, beam retains positive slope.

is removed from the resonance region, and it was assumed that $\gamma \approx \gamma_p$. The numerical value from the seven experiments was $\Delta E_b \approx 3.9 W_{R, \max}$. The knowledge of $W_{R, \max}$ as a function of γ allows us to divide the beam parameter region into two regimes (Fig. 5). If $W_{R, \max}$ is greater than the energy level for quasilinear stabilization ($\approx E_b/3$),

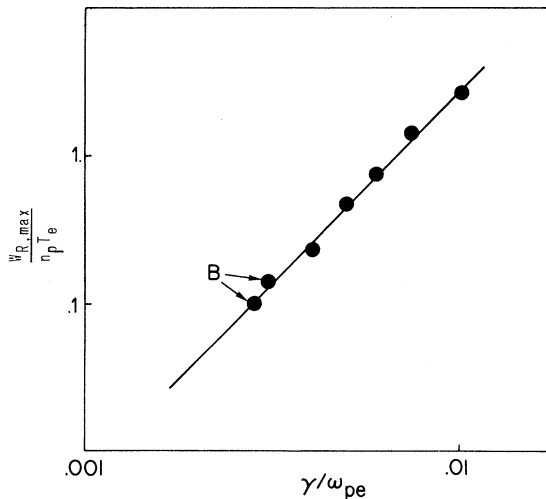


FIG. 4. Results of a series of computer simulations. Shown is the maximum energy of resonance beam waves vs growth rate.

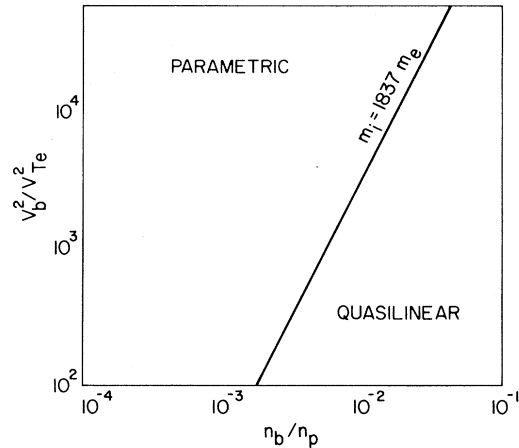


FIG. 5. Determined from simulations parameter regimes in which kinetic beam instability will stabilize parametrically or quasilinearly.

the beam will relax quasilinearly; otherwise it will stabilize parametrically before plateau formation.

In this Letter we have shown that parametric instabilities can prevent plateau formation in a warm-beam-plasma interaction, and presented the scalings with respect to beam energy loss ΔE_b and $W_{R, \max}$. The main observables of the nonlinear stabilization are as follows: (1) reduction in the coupling between the warm beam and the background plasma, over that expected from quasilinear theory; (2) beam-type structure existing for longer times or propagating greater distances in an ambient plasma; (3) generation of short-wavelength electric fields with phase velocities much below the streaming velocity of the beam; (4) superthermal electron tails both parallel and counterstreaming to the beam; (5) enhanced low-frequency ion fluctuations.

The results presented here apply only to the initial stabilization of the beam-plasma interaction. The long-term nonlinear stabilization is presently being studied.

We wish to acknowledge useful discussions with Dr. D. Book, Dr. J. Orens, and Dr. P. Palmadesso. This work was supported by the Office of Naval Research.

¹R. C. Davidson, *Methods in Nonlinear Plasma Theory* (Academic, New York, 1972), pp. 174-197.

²B. N. Breizman and D. D. Ryutov, *Nucl. Fusion* **14**, 873 (1974).

³K. Papadopoulos, M. Goldstein, and R. Smith, *Astro-*

phys. J. 190, 175 (1974).

⁴K. Papadopoulos, Phys. Fluids 18, 1769 (1975).

⁵P. J. Palmadesso, T. P. Coffey, I. Haber, and K. Papadopoulos, Bull. Am. Phys. Soc. 20, 1277 (1975).

⁶K. Papadopoulos and T. Coffey, J. Geophys. Res. 79, 674 (1974).

⁷D. Hammer and K. Papadopoulos, Nucl. Fusion 15, 977 (1975).

⁸R. L. Morse and C. W. Nielson, Phys. Fluids 12, 2418 (1969).

⁹D. Biskamp and H. Welter, Nucl. Fusion 12, 89

(1972).

¹⁰S. Kainer, J. Dawson, and T. Coffey, Phys. Fluids 15, 2419 (1972).

¹¹Lester E. Thode and R. N. Sudan, Phys. Fluids 18, 1552 (1975).

¹²J. M. Dawson and C. Oberman, Phys. Fluids 5, 517 (1962).

¹³D. F. DuBois and M. V. Goldman, Phys. Rev. Lett. 19, 1105 (1967).

¹⁴A. A. Ivanov and L. I. Rudakov, Zh. Eksp. Teor. Fiz. 51, 1522 (1966) [Sov. Phys. JETP 24, 1027 (1967)].

Effects of Elliptically Polarized Shear Flows in Nematics

Pawel Pieranski and Etienne Guyon

Laboratoire de Physique des Solides, Université Paris-Sud, 91405 Orsay, France

(Received 28 July 1977)

We report the observation of an instability pattern in a homeotropically oriented nematic slab subject to elliptically polarized shear flow, a phenomenon which we explain as resulting from nonzero time-averaged Leslie-Ericksen viscous stresses.

In nematics, steady (that is to say nonzero time-averaged) forces, torques, and velocities in an alternating flow have often been interpreted as being due to acoustical streaming, the phenomenon related to second-order nonlinear terms such as $\langle \rho(\vec{v} \cdot \nabla)\vec{v} \rangle$ where \vec{v} is the alternating velocity and ρ the density. Nagai *et al.*¹ and Miyano and Shen¹ give typical examples of such an approach as well as an exhaustive review of previous contributions to the acoustic effects in nematics. Apart from the force density resulting from ordinary radiation pressure in absorptive medium, one has other effects due to the anisotropy of the liquid crystals.²

The aim of this Letter is to illustrate the following fact: In nematics, the ordinary viscous stresses [a typical term has the form³ $\alpha_s \vec{n}(\vec{n} \cdot \hat{A})$ where $A_{ij} = \frac{1}{2}(\partial_i v_j + \partial_j v_i)$], which are *explicitly* first order in the velocity gradients (as in isotropic Newtonian fluids), are also a function of the molecular orientation \vec{n} . In alternating flows, \vec{n} varies periodically together with the velocity \vec{v} so that there is an *implicit* nonlinearity. Consequently, viscous stress can be considered as another source of steady forces, torques, and velocities. Our point of view is based on the study of the effects of the elliptically polarized shear flow which we report and explain here.

In general, an elliptically polarized signal can be constructed from two orthogonal (along x and y) linearly polarized signals (the principal axes are

not along x and y in general).

Our observations were performed with the flow cell shown in Fig. 1. The elliptical shear is produced by applying to the two parallel glass plates, G_x and G_y , containing the homeotropic liquid crystal, linearly polarized displacements $x = x_0 \sin \omega t$, $y = y_0 \cos \omega t$. For the frequencies used (100 Hz $< f < 500$ Hz, with $f = \omega/2\pi$) the viscous penetration depth $\delta_{\text{visc}} = (2\nu/\omega)^{1/2} \approx 200 \mu\text{m}$ is larger than the thickness of the sample so that the alternating shear, of the form $s_x = s_{x_0}^a \cos \omega t = (x_0 \omega/d) \cos \omega t$,

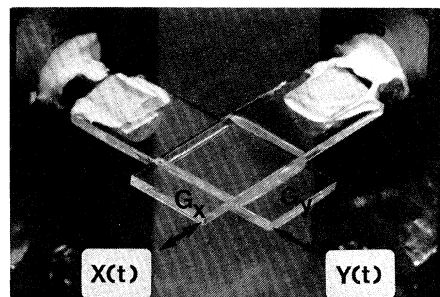


FIG. 1. The flow cell is made up of two glass plates G_x and G_y which partially overlap. The nematic liquid crystal (N-[*p*-methoxybenzylidene]-*p*-butylaniline), held by capillary action in the gap, is oriented homeotropically by surface treatment ($\vec{n} \parallel z \perp G_{x,y}$). The two glass plates are attached to two mechanically independent systems which allow adjustment of the thickness d and parallelism. Oscillatory displacements of the two plates are induced by applying ac voltages to loudspeaker elements to which the plates are attached.